Atmos. Chem. Phys. Discuss., 13, 28819–28868, 2013
www.atmos-chem-phys-discuss.net/13/28819/2013/
doi:10.5194/acpd-13-28819-2013

Atmospheric Chemistry and Physics Discussions

The effect of atmospheric aerosol particles and clouds on Net Ecosystem Exchange in Amazonia

G. G. Cirino[1], R. F. Souza[2], D. K. Adams[3], and P. Artaxo[4]

[1]National Institute of Research in Amazonia, Rua André Araujo, 2936, LBA, 60060-000, Manaus, AM, Brazil
[2]State University of Amazonas, Av. Darcy Vergas, 1200, 69065-020, Manaus, AM, Brazil
[3]Centro de Ciencias de La Atmósfera, Universidad Nacional Autónoma de México, Circuito Exterior s/n, Ciudad Universitaria, Del. Coyoacán, 04510, D.F, Mexico
[4]Institute of Physics, University of São Paulo, Rua do Matão, Travessa R, 187, 05508-090, São Paulo, SP, Brazil

Received: 29 August 2013 – Accepted: 29 September 2013 – Published: 5 November 2013

Correspondence to: G. G. Cirino (glauber.cirino@inpa.gov.br)

Published by Copernicus Publications on behalf of the European Geosciences Union.

Abstract

Carbon cycling in Amazonia is closely linked to atmospheric processes and climate in the region as a consequence of the strong coupling between the atmosphere and biosphere. This work examines the effects of changes in net radiation due to atmospheric aerosol particles and clouds on the Net Ecosystem Exchange (NEE) of CO_2 in the Amazon region. Some of the major environmental factors affecting the photosynthetic activity of plants, such as air temperature and relative humidity were also examined. An algorithm for clear-sky irradiance was developed and used to determine the relative irradiance *f*, which quantifies the percentage of solar radiation absorbed and scattered due to atmospheric aerosol particles and clouds. Aerosol optical depth (AOD) was calculated from irradiances measured with the MODIS (Moderate Resolution Imaging Spectroradiometer) sensor, onboard the TERRA and AQUA satellites, and was validated with ground-based AOD measurements from AERONET sun photometers. Carbon fluxes were measured using eddy-correlation techniques at LBA (The Large Scale Biosphere–Atmosphere Experiment in Amazonia) flux towers. Two sites were studied: the Biological Reserve of Jaru (located in Rondonia) and the Cuieiras Biological Reserve (located in a preserved region in central Amazonia). In the Jaru Biological Reserve, a 29 % increase in carbon uptake (NEE) was observed when the AOD ranged from 0.10 to 1.5. In the Cuieiras Biological Reserve, this effect was smaller, accounting for an approximately 20 % increase in NEE. High aerosol loading (AOD above 3 at 550 nm) or cloud cover leads to reductions in solar flux and strong decreases in photosynthesis up to the point where NEE approaches 0. The observed increase in NEE is attributed to an enhancement (∼50 %) in the diffuse fraction of photosynthetic active radiation (PAR). Significant changes in air temperature and relative humidity resulting from changes in solar radiation fluxes under high aerosol loading were also observed at both sites. Considering the long-range transport of aerosols in Amazonia, the observed changes in NEE for these two sites may occur over large areas in Amazonia, significantly altering the carbon balance in the largest rainforest of the world.

1 Introduction

Clouds and aerosols influence both the surface energy balance and hydrological cycle through the modification of incoming solar radiation flux and precipitation (Benner and Curry, 1998; Gu et al., 1999, 2001). Consequently, clouds and aerosols exert direct influence on terrestrial ecosystems and are, therefore, expected to modify CO_2 exchanges in the biosphere–atmosphere interface. Over the past 20 yr, field observations over many regions, have shown that the highest rates of carbon uptake in forest ecosystems often occur on slightly cloudy rather than sunny days (Gu et al., 1999; Law et al., 2002; Yamasoe et al., 2006; Oliveira et al., 2007; Jing et al., 2010). Other studies have found that for a given level of irradiance, cloudy days, compared to clear days, generally have higher absolute values of Net Ecosystem Exchange (NEE) (Baldocchi, 1997; Goulden et al., 1997; Gu et al., 1999; Doughty et al., 2010) due to the increase in diffuse radiation, except for highly overcast conditions. Several mechanisms have been proposed to explain these observations including: increases in diffuse radiation (Gu et al., 1999; Yamasoe et al., 2006; Oliveira et al., 2007; Mercado et al., 2009; Jing et al., 2010; Zhang et al., 2010), reduced respiration of sunlit leaves (Baldocchi, 1997; Miller et al., 2004; von Randow et al., 2004), reduction in water vapor pressure difference (VPD) and, finally, modifications in stomatal dynamics associated with ambient light fluctuations. Although these observations have been limited to flux tower measurements (i.e., a few point measures), it is expected that an increase in carbon uptake under increasing cloudiness and atmospheric aerosol load has implications for regional and global climate (Abakumova et al., 1996; Gu et al., 1999). This is of particular interest for regions where the percentage of cloud cover and vegetated areas have increased recently (Keeling et al., 1996; Myneni et al., 1997; Gu et al., 1999, 2003).

Long-term studies coordinated by the LBA experiment (The Large Scale Biosphere–Atmosphere Experiment in Amazonia) have shown that total annual emissions of CO_2 derived from land use change are between 150 and 200 megatons of C per year (Houghton et al., 2000). On the other hand, studies of forest inventories (Phillips et al.,

1998) indicate that intact Amazonian forest may represent a sink of carbon at rates ranging from 0.5 up to a high value of $7\,tC\,ha^{-1}$ annually (Araújo et al., 2002; Ometto et al., 2005; Malhi, 2010, 2012). Although there is a significant uncertainty regarding the role of the Amazon as a sink or as a source of carbon to the atmosphere (Keller et al., 1996), due to the balance between deforestation and biomass burning emissions vs. enhanced carbon uptake, recent numbers indicate a kind of balance in uptake/emissions. In Amazonia, biomass burning is the main driver of changes in atmospheric composition, accounting for a significant increase in the concentration of gases and particles in the dry season (Artaxo et al., 2002, 2009; Davidson et al., 2012). This translates into a large anthropogenic impact on the local energy balance, and brings important environmental consequences for the entire Amazon ecosystem (Artaxo et al., 1998; Schafer et al., 2002; Procopio et al., 2004; Sena et al., 2013). In the dry season, where biomass burning emissions are widespread, the reduction in the ground-based flux of photosynthetic active radiation (PAR) can reach values of the order of 70 % (Eck et al., 2003; Procopio et al., 2004), strongly impacting Amazon rainforest primary production (Artaxo et al., 2013). This augmented aerosol loading boosts the fraction of diffuse radiation in the atmosphere, which, in turn, increases the penetration of solar radiation into the forest canopy. The vegetation uses diffuse radiation more efficiently for photosynthesis, which increases forest carbon uptake; a fact that partly balances the effects of reducing direct radiation flux. Most of the Amazon, even outside the region of the so-called "arc of deforestation" experiences the effects of biomass burning emissions to some extent, with the resulting modification in the ecosystem functioning (Oliveira et al., 2007; Doughty et al., 2010; Artaxo et al., 2013).

Atmospheric aerosol lifetime is of the order of days to weeks and thus long-range transport of aerosol particles implies that biomass burning may impact the radiation budget of areas thousands of kilometers away (Seinfeld and Pandis, 2006; Martin et al., 2010b). More knowledge is needed with respect to the impacts that clouds and aerosols have on carbon absorbed by the Amazon forest annually, especially in regions of the Central Amazon, which suffer smaller impacts from biomass burning emissions.

CO_2 flux monitoring has been limited essentially to 13 flux towers distributed over 5.5 million km^2 and operated by the LBA experiment. Given this observational density and length of record (~ 10 yr), it has not been possible to draw conclusions about clouds and aerosols impacts on the carbon cycle for Amazonia. Moreover, the limited number of sun-photometers for continuous monitoring of aerosol optical depth at these flux tower sites, especially in the central Amazon, has greatly hampered a broader and more precise mapping of the relationship between biomass burning aerosols and the net balance of carbon in the Amazonian forest. A few previous studies have shown a significant relationship between fluxes and aerosols in Amazon, but these were made from relatively short data time series and are representative of only two regions of the Amazon: Rondonia-RO and Santarem-PA (Yamasoe et al., 2006; Oliveira et al., 2007; Doughty et al., 2010).

In the present study, the influence of clouds and aerosol particles emitted by biomass burning on the NEE for two sites in Amazonia was analyzed. Furthermore, the net effect of the increase in diffuse radiation fraction and the reduction of the total solar flux on carbon fluxes were analyzed. This analysis was carried out using long-term LBA meteorological and eddy-correlation flux data, in addition to Aerosol Optical Depth (AOD) measurements from MODIS (Moderate Resolution Imaging Spectroradiometer). Moreover, our study implies that the use of remotely sensed AOD can be expanded into forested regions where there are no solar photometry AERONET (Aerosol Robotic Network) sites, thus enabling a broader mapping of the net exchange of carbon between the forest canopy and the atmosphere.

2 Data and measurement

2.1 Site descriptions

Two LBA flux tower sites were chosen for this study, both having long-term measurements of carbon flux, aerosol optical depth, radiation and vertical profiles of CO_2, temperature and relative humidity within the canopy. Separated by approximately 1000 km, each site experiences a different precipitation regime and nearby land-use activities. The Forest Reserve of Jaru – RBJ is a protected area located in southeastern Rondonia and is strongly affected every year by biomass burning emissions (Andreae et al., 2004; Oliveira et al., 2007; Silva Dias et al., 2002). Previous studies have shown strong seasonality and carbon assimilation, around −18 and −8 kg C ha^{-1} day^{-1} during on the wet and dry season, respectively (von Randow et al., 2004). At this site, this study analyzed approximately 4 yr of measurements of carbon flux and associated meteorological variables (March 1999 to November 2002). The second LBA site (Cuieiras Forest Reserve), located in Central Amazonia 60 km northwest of Manaus, was chosen as representative of an intact, well-preserved forest site with little disturbance or deforestation in recent decades. In the Cuieiras Reserve, the seasonal variations in net carbon uptake by the ecosystem are small (de Araujo et al., 2002, 2010). At this site, this work has analyzed a long time series (~ 10 yr) of carbon flux and meteorological variables, between June 1999 and December 2009. Figure 1 shows the locations of the two sites used in this study.

2.1.1 Jaru Biological Reserve (RBJ)

The Biological Reserve of Jaru (10°05′00″ S and 61°55′00″ W) is densely forested and located approximately 100 km north of the urban area of Ji-Parana, Rondonia, Brazil. It consists of approximately 268 000 ha of primary forest at an altitude ranging between 100 and 150 m a.s.l. with typical canopy height of 30–35 m. Although the forest reserve is protected by Brazilian Environmental Protection Agency (IBAMA), in recent years it has suffered from forest fires and deforestation relatively close to the sampling site (von Randow et al., 2004). The different geological substrates and diverse rainfall patterns at this site promote numerous vegetation types and five phyto-ecological formations, namely: Open Tropical Rain Forest, Rain Forest, Vegetation Transition or Contact, Cerrado and Alluvial Pioneer Formations. Average annual rainfall ranges from 1400–2600 mm yr^{-1} with the dry season (rainfall < 60 mm per month) extending from

June to September (Machado et al., 2004; da Rocha et al., 2009). The average annual air temperature is about 24–26 °C, with average relative humidity being around 90 %, although dropping to around 40 % in August. During the dry season, weak cold fronts locally called "friagens", can also lower temperatures substantially (~ 15 °C) (Fisch et al., 1998).

2.1.2 Cuieiras Biological Reserve (K34)

The second sampling site is the so-called K34 LBA tower flux, located in the central Amazon's Cuieiras Biological Reserve (2°36′32.67″ S, 6°12′33.48″ W). The K34 tower has been widely utilized for over 10 yr for a range of meteorological studies, inluding energy and trace gases fluxes (de Araujo et al., 2002, 2010) and even tropospheric variables such as precipitable water vapor (Adams et al., 2011). The study area is densely forested with typical canopy height of 30 m with significant variation (20–45 m) throughout the Reserve. Topography is complex containing a sequence of plateaus, hills and lowlands. The topography of this site, which has a maximum altitude of 120 m, is distributed between 31 % plateau, 26 % slope and 43 % valley (Rennó et al., 2008). More detailed characteristics of the soil in this region can be found in Ferraz et al. (1998); Higguchi et al. (1998) and Oliveira and Amaral (2005). The climate is characterized by an average annual temperature of 26.0 °C, with minimum and maximum values of 23.5 °C and 31.0 °C, respectively, and an average annual relative humidity of 84 %. The average annual precipitation is approximately 2300 mm. Although rainfall can occur in any month of the year, the annual cycle of precipitation is characterized by a punctuated wet season from January to April and a strong dry season from July to September. The dry season (rainfall less than 100 mm) can also vary from year-to-year in length (da Rocha et al., 2009).

2.2 Measurements

2.2.1 Meteorological and flux measurements of CO_2

In this study, a long time series of flux measurements of CO_2 and meteorological variables are used. Our database includes measurement of the net flux of CO_2 (NEE), obtained using eddy correlation techniques and micrometeorological measurements (1999 to 2009), derived from automatic weather stations (Automatic Weather Stations – AWS) distributed vertically along the tower. Micrometeorological measurements and carbon fluxes were recorded by data loggers at different time steps and were averaged for every 30 to 60 min. AWS stations are comprised of a set of instruments and sensors for measuring solar radiation (0.3–3 µm), thermal radiation (4.5–42 µm) and reflected radiation (all to within ±1 %), a net radiometer to measure net radiation, wet and dry bulb thermometers (±0.1 °C), anemometers with a minimum wind speed of 0.3 to 0.4 m s^{-1} and a rain gauge with accuracy of ±0.2 mm. The vertical profile of CO_2 concentrations between the soil and atmosphere were obtained using a closed path infrared gas analyzer. The fluxes of H_2O and CO_2 were performed through the eddy covariance system similar to that described by Moncrieff et al. (1997). The system is comprised of a sonic anemometer (~ 10.4 Hz), and an infrared gas analyzer. Fluxes, means and variances were averaged every 30 min, with data processed using Alteddy (version 3.1) based on Aubinet et al. (2000). Table 1 contains a detailed list of the sensors employed. The instrumentation and data acquisition systems are similar at both study sites. However, the procedures for data collection, calibration of sensors, and other operational issues do differ to a small extent between the two sites. The data collection heights can be seen in Table 1 as well as canopy heights for both sites.

2.2.2 Measurements of Aerosol Optical Depth

Remotely sensed aerosol optical depth measurements at 550 nm are taken from two sources, the MODIS instrument on Aqua and Terra platform (MODIS Atmosphere Prod-

ucts, MOD/MYD-04L2) and from the solar radiometer network AERONET (Aerosol Robotic Network). The CIMEL CE 318-A radiometers have detectors capable of performing direct solar radiation as well as almucantar measurements (Holben et al., 1998). Direct solar measurements have a field of view of 1.2° for eight spectral bands centered at 340, 380, 440, 500, 670, 870, 940 and 1020 nm, determined by rotational interference filters located within the sensor. Each measurement takes approximately 10 s. In this study, the AERONET measurements were considered the standard measurement of AOD and used only to validate the MODIS retrieved AOD. MODIS AOD was calculated from February 2000 to September 2010 (at the RBJ site) and February 2000 to November 2002 (at the K34 site). In order to minimize cloud contamination issues, only AERONET, level 2.0 AOD data were used in the comparison with MODIS AOD. The remotely sensed estimations of AOD are typically made daily between 09:30 a.m. to 11:55 a.m. (Local Time, LT) in the case of MODIS-Terra, and between 12:40 to 14:55 (LT) in the case of MODIS-Aqua. For consistent comparisons between the estimates of AOD (MODIS) and AERONET, only the radiation flux between solar zenithal angles from 10 to 55° were considered. The number of days with AOD data were maximized by combining the estimates from both the Terra and Aqua satellites. These estimates are averages of an area of $50 \times 50\,km^2$ collocated with the LBA flux towers. Periods when either measurements of CO_2 (eddy flux) or MODIS AOD were absent were not employed in this study.

2.3 Methods

In this section, a description of the procedures employed to observe aerosol and clouds effects on net radiation fluxes is provided. Firstly, the variables used to estimate the cloudiness are presented. In meteorological observations, the cloudiness is usually measured in tenths or eighths of sky covered. However, in the present study, the word "cloud" will be used to refer to the presence, quality or quantity of clouds in the sky. A method to identify clear-sky conditions was also developed. The procedures used

to evaluate cloud/aerosol influence on NEE including the environmental factors that possibly contribute to changes in the carbon flux are also described.

2.3.1 Calculation of net ecosystem CO_2 exchange

At both sites, NEE is obtained from turbulent flux measurements by means of the eddy covariance technique taking into account the storage term (de Araújo et al., 2010; von Randow et al., 2004). Micrometeorological sensors distributed vertically along the tower are essential for the NEE calculations (Richardson and Hollinger, 2005), using continuous measurements of the CO_2 profile between soil and top of the tower. Under these conditions, NEE can be approximated by:

$$\mathrm{NEE} \approx \mathrm{Fc} + \mathrm{Stg} \quad (1)$$

Where Fc is called "CO_2 turbulent flow", calculated by the eddy correlation system above the treetops; Stg (the storage term) is the CO_2 concentration (non-turbulent term), measured in a vertical profile at discrete levels z_i of Δz_i thickness, from the soil surface to the point of eddy correlation measurements around 53 m and 63 m on the K34 and RBJ towers, respectively (Finnigan, 2006; Loescher et al., 2006; Dolman et al., 2008). At RBJ, procedures for calculating the NEE were made following von Randow et al. (2004). At K34, vertical profiles of CO_2 concentrations were calculated following Albinet et al. (2001) and de Araujo et al. (2010).

$$\mathrm{Stg} = \frac{P_a}{RT_a}\int_0^z \left(\frac{\partial c}{\partial t}\right)\partial z \quad (2)$$

Where P_a is the atmospheric pressure ($N\,m^{-2}$), R is the molar gas constant ($N\,mmol^{-1}\,K^{-1}$), T_a is the air temperature (K), c is the [CO_2] ($\mu mol\,mol^{-1}$), t is the time (s) and z is the maximum height (m) between the ground and the canopy (Finnigan, 2006; Loescher et al., 2006).

Figure 2 shows the diurnal cycle of NEE during the wet and dry season at both sites. The diurnal cycle of NEE is typical for tropical forests, with the magnitudes and peak hours of carbon absorption (Table 2) consistent with previous observations in other areas of the Brazilian Amazon forest (de Araujo et al., 2010; Hutyra et al., 2008; von Randow et al., 2004; Vourlitis et al., 2011). NEE is negative during daytime when photosynthesis is larger than respiration. During nighttime, CO_2 fluxes are predominantly positive and CO_2 is released into the atmosphere (respiration greater than photosynthesis). Differences in respiration values between the two locations are associated with both the intrinsic physiological characteristics of both ecosystems as well as issues associated with the topographic complexity in the Manaus K34 area (von Randow et al., 2004; Tota et al., 2008; de Araujo et al., 2010; Mahrt, 2010). It was also possible to observe over the dry season that the maximum carbon absorption (negative values) does not occur at local solar noon, but often around 10:00 LT, at both sites. On the other hand, during the wet season, the maximum negative values of NEE were observed around 11:00–12:00 LT. This indicates a possible connection between biotic and physical factors with a possible ecophysiological response of vegetation to higher availability of incoming radiation in the dry period (da Rocha et al., 2004, 2009; de Araujo et al., 2010). Large variability in CO_2 fluxes during the first hours of the day, with larger standard deviations compared to nighttime values were observed (Fig. 2). This is due to early morning turbulence at the canopy level and the breakup of the nocturnal boundary layer and the beginning of the daytime boundary layer (Betts and Dias, 2010).

2.3.2 Procedure for the quantification of aerosol and clouds effects on NEE

Since no direct observations of cloud cover were made at K34 or RBJ, measurements of global solar radiation at the surface to assess the presence or absence of clouds were used (Gu et al., 1999; Oliveira et al., 2007; Zhang et al., 2010; Bai et al., 2012). The critical step in this approach is to identify what is a "clear-sky" day in order to establish a basis for comparison with cloudy or partly cloudy days. In the present study, the words "cloud" or "cloudiness" was used to refer to the presence, without regard for

quality or quantity, of clouds in the sky (Gu et al., 1999). The concept of relative irradiance, f, was used to determine the reduction of incident solar irradiance due to clouds and/or aerosols and associate this with the changes in NEE, which also changes with temperature and relative humidity variations. In this study, the quantity f was calculated following Oliveira et al. (2007):

$$f = \frac{S\{\mathrm{AOD}, \mathrm{cloudiness}\}}{S_0\{\mathrm{AOD}_{0.10}, \mathrm{cloudless}\}} \times 100 \quad (3)$$

Where S (W m^{-2}) is the total incident solar radiation measured on the surface at a given time (with or without the presence of aerosols and clouds) and S_0 (W m^{-2}), the expected total incident solar irradiance at the surface in a cloudless atmosphere with an aerosol optical depth of 0.10 at 550 nm. Previous studies in Amazonia have shown that the background AOD, due to atmospheric natural conditions is about 0.1 at 550 nm (Holben et al., 1996; Guyon et al., 2003). There are few models assessed in the literature for the calculation of S_0 (Ricchiazzi et al., 1998; Duchon and O'Malley, 1999). In this study, we chose to employ an algorithm for clear-sky irradiance that would include the intrinsic characteristics of local conditions in the Amazon. S_0 and f were calculated employing the methodology of Gu et al. (1999), which establishes a set of criteria to find clear-sky days. These criteria are based on the concept of clearness index, kt, which is discussed in detail in the next section. In this study, kt was used to find S_0 and thus determine f. To observe only the aerosol effect on the solar irradiance flux (computed from f), and consequently on the NEE measurements, the aerosol effect has to be isolated from the cloud effect. Radiation measurements were classified as affected only by aerosols if they were performed under cloudless conditions, that is, under clear-sky conditions (Oliveira et al., 2007). The MODIS sensor has a reasonable algorithm to exclude cloud contamination of the AOD measurements (King et al., 1999, 2003; Remer et al., 2005).

2.3.3 The definition of the clearness index

The relative irradiance, f, provides an estimation of changes in cloudiness and AOD as a result of changes in measured solar radiation fluxes. However, the concept requires that S_0 be available. When clear-sky irradiance is not available, sky conditions can be described in terms of the "clearness index", kt, defined as the ratio of solar radiation received at the surface to the solar irradiance at the top of the atmosphere (TOA). For a given solar elevation angle, small kt values indicate an increase in the cloud coverage and/or aerosol loading, while higher values indicate more clear sky conditions (Gu et al., 1999; Zhang et al., 2010; Bai et al., 2012). Mathematically, the clearness index can be expressed by:

$$\mathrm{kt} = S/S_{\mathrm{e}} \tag{4a}$$

$$S_{\mathrm{e}} = S_{\mathrm{sc}}\left[1 + 0.033\cos\left(\frac{360\,\mathrm{td}}{365}\right)\right]\sin\beta \tag{4b}$$

Where S is the ground-based total solar irradiance actually measured at the surface, while S_{e} is the TOA solar irradiance, where S_{sc} ($\sim 1367\,\mathrm{W\,m^{-2}}$) is the solar constant, and td the Julian Day. For the calculation of $\sin\beta$ the following equation is used:

$$\sin\beta = \sin\varphi\cdot\sin\delta + \cos\varphi\cdot\cos\delta\cdot\cos\omega \tag{5}$$

Where (β) is the solar elevation angle and (ϕ), (δ) and (ω) are, respectively, the latitude, the declination of the Sun (in degrees) and the hour angle. An interesting characteristic of this definition is that it is possible establish a clearness index for clear skies (i.e., cloud free and AOD $\sim$ 0.10). Under these conditions, it is possible to denominate a clear-sky clearness index, kt*, and Eq. (4a) can be rewritten as:

$$\mathrm{kt}^* = \frac{S_0}{S_{\mathrm{e}}} \tag{6}$$

Therefore, the ratio between kt and kt* provides the relative irradiance f; see Eq. (3). The physical concepts of kt and kt* indicate an alternate way to determine f to a good approximation.

2.3.4 Defining clear skies conditions

To quantify the specific influence of clouds on NEE, firstly, the NEE behavior on days with minimal cloud cover was determined using the method of separation of clear days from Gu et al. (1999). This provides a basis for the comparison of NEE behavior for "clear-sky days" vs. aerosol and/or cloudy days. The "clear-sky" days were defined based on a 4 h period, evaluated for two temporal intervals: between 08:00 a.m. to 12:00 p.m. and from 12:00 p.m. to 04:00 p.m., local time (averages were made of the irradiances over each 4 h period). These periods were used because of the timing of the close overpass of the Aqua and Terra satellites over Amazonia. To ascertain the accuracy of our cloudiness estimates with an independent data set, time-averaged GOES10 channel 4 brightness temperature was used over the same two 4 h periods for the pixel (4 km × 4 km) containing the K34 and RBJ sites. Brightness temperatures less than 280 K were assumed to result from cloudiness for that particular pixel. The clear days selected by the method of Gu (1999) were compared with the clear sky days from satellite observations (GOES10) and it was found that about 70 % of the number of clear days selected by GOES10 were also selected by the method of Gu (1999).

Two patterns for clear mornings and afternoons were assumed (Gu et al., 1999; Zhang et al., 2010; Bai et al., 2012): (1) kt should increase smoothly with the solar zenith angle – cos(z) and (2) the relationship between clear-sky kt and cos(z) must form an envelope in the "lumped" scatterplot of kt against cos(z). The following steps and procedures were employed to find kt*: First, value of kt were plotted against time of the day. Only the mornings and afternoons that showed small variations in kt were selected. The solar zenith angle cos(z) from the "clear-sky days" were ploted on the same graph. The kt values which were outside the two patterns set out above were excluded from our database. Finally, the values of kt found during the mornings and

afternoons clear-sky selected were plotted with the solar zenith angle again to check if the clear-sky days selected met the two criteria set out above.

The degree of dependence between kt^* (clear-sky clearness index) and $\cos(z)$ was used to assess whether the mornings and clear afternoons were accurately selected. This relationship can be expressed as follows:

$$kt_0 = a_1\cos^3(z) + a_2\cos^2(z) + a_3\cos(z) + a_4 \quad (7)$$

Where kt_0 is the clear-sky clearness index from the regression curves (Fig. 3a and b); z is the solar zenith angle calculated Gates (1980); a_1, a_2, a_3 and a_4 are the regression coefficients specific to the selected clear mornings and afternoons, calibrated to local conditions of the tropical forest at K34 and RBJ, respectively. The clear-sky irradiance (S'_0) was also determined, obtained similarly to Eq. (7). The coefficients kt_0 and S'_0 are fixed as showed in Table 3.

Figure 3 show asymmetries between the period of morning and afternoon light at both sites. The values of kt^* selected during afternoons are slightly higher when compared with the indexes of selected mornings, especially for low angles (less than $\cos^{-1}$ 0.45). Similar results were obtained by Gu et al. (1999) and Zhang et al. (2010). For a given solar zenith angle, decreases in the clearness index generally indicate an increase in the depth of the clouds, with the exception for situations in which the clouds are not distributed uniformly across the sky; i.e., when there is a cloud gap effect (Gu et al., 1999; Oliveira et al., 2007).

2.3.5 Determination of NEE on clear-sky days

In this study, the influence of aerosols and clouds on carbon uptake is analyzed mainly in terms of variations in NEE and environmental factors through their impact on f. The observed NEE on clear days was used also as a basis of comparison for cloudy days and/or days with high aerosol loading. Equation (1) and NEE (clear-sky) were used to calculate the percentage effect of aerosols and clouds on the carbon flux (%NEE) by

way of the following relationship (Gu et al., 1999; Oliveira et al., 2007; Bai et al., 2012):

$$\%NEE = \left(\frac{NEE(z) - NEE(z)_{csky}}{NEE(z)_{csky}}\right) \times 100 \quad (8)$$

Where $NEE(z)$ is a measure of NEE under a given condition sky throughout the day and NEE_{csky} is the NEE calculated under sky conditions with low aerosol loading in the atmosphere and minimal cloud cover ($f \approx 1.0$, AOD ~ 0.10).

To eliminate the interference of sun elevation angle on the variation of NEE% or NEE on the relative irradiance parameter f, data grouped at intervals of solar zenithal angle between 10–20 and 20–35 were initially analyzed. Zenith angles of 5° intervals proved too small to develop a robust statistical analysis (Gu et al., 1999). Values above 50° or around 0° (solar angle very near the horizontal and vertical plane, respectively) were in general too heavily contaminated by clouds. Therefore, a 10 to 35° elevation angle was chosen to be optimal for measuring the ecosystem response to changes in cloudiness and AOD rather than the effect of variations in solar zenith angles.

The results shown in Fig. 4a and b show the solar zenith angle interval for which carbon fluxes experiences the greatest variation. The statistical parameters R^2 and p value (Fig. 4a and b) are satisfactory in view of the measurement sample size; For K34 > 59 000 points, and for RBJ > 26 000 values. The coefficient of determination R^2 is relatively low, but the level of statistically significant p values in all cases are smaller than 0.001, indicating a high degree of relationship between the NEE and solar zenithal angle. The obtained coefficients of NEE (clear-sky) are listed in Table 4. These coefficients are consistent with those of the Tapajos National Forest in Amazonia, reported by Oliveira et al. (2007), but are quite different from those obtained in other ecosystems, such as temperate deciduous forests, mixed forests and pine forest, found in southern Canada and Northwest China, respectively (Gu et al., 1999; Zhang et al., 2010).

The relationship between NEE and some variables that directly interferes with the uptake of carbon by forests, such as: total PAR, diffuse PAR, air temperature, canopy temperature and VPD were also studied. This discussion about methods used to calcu-

late total PAR downward radiation, diffuse PAR and canopy temperature are discussed in Sects. 2.3.6 and 2.3.7.

2.3.6 Methods to derive total and diffuse PAR

Unfortunately, measurements of diffuse PAR, were not available at either K34 or RBJ. Therefore, to determine the diffuse component of total PAR, we followed the methods derived by Spitters et al. (1986) and Reindl et al. (1990) which have been widely used in the literature (Gu et al., 1999; Jing et al., 2010; Zhang et al., 2010; Bai et al., 2012). The calculation is performed deriving the diffuse PAR radiation PARf from the following formulation (Spitters, 1986):

$$\mathrm{PAR_f} = \left[\frac{[1+0.3(1-q^2)]q}{1+(1-q^2)\cos^2(90^\circ - z)\cos^3 z}\right] \times \mathrm{PARt} \quad (9)$$

Where $\mathrm{PAR_f}$ is the diffuse PAR radiation ($\mu\mathrm{mol\,photon\,m^{-2}\,s^{-1}}$) and $q = (S_f/S_e)/\mathrm{kt}$; S_f denotes the total diffuse radiation (visible plus near infrared) received on a horizontal plane at the Earth's surface ($\mathrm{W\,m^{-2}}$). The fraction of diffuse PAR was defined as the ratio between $\mathrm{PAR_f}$ and total PAR (PARt). To express the light use efficiency (LUE) of vegetation and the fraction of diffuse PAR (D_f), respectively, the NEE and $\mathrm{PAR_f}$ values were normalized by PARt as follows (Jing et al., 2010):

$$\mathrm{LUE} = \mathrm{NEE}/\mathrm{PARt} \quad (10)$$

$$D_f = \mathrm{PAR_f}/\mathrm{PARt} \quad (11)$$

2.3.7 Canopy top temperature

As there are no direct measurements of skin temperature of the canopy at either study sites, we used the data sets of pyrgeometers operated around 15–20 m high inside the canopy on both sites (Table 1) to measure the emission of long wave radiation from the

surface ($L\uparrow$) ($\mathrm{W\,m^{-2}}$). The Eq. (11) was derived from the Stefan–Boltzmann equation and used to calculate the temperature of the canopy (T_c) of the K34 and RBJ sites K34. Dougthy et al. (2010) used similar procedures to estimate the canopy temperature (skin temperature) in FLONA-Tapajos (Santarem-PA).

$$T_c = \left(\frac{L\downarrow}{\sigma\varepsilon}\right)^{0.25} \quad (12)$$

Where ε is the emissivity, assumed 0.98 (Monteith and Unsworth, 1990) and σ the Stefan–Boltzmann constant ($5.670 \times 10^{-8}\,\mathrm{W\,m^{-2}\,K^{-4}}$).

3 Results and discussions

This section presents and discusses the main results of this study. The first task was to validate MODIS AOD estimations with the AOD measurements from the AERONET sun-photometer network. Following this, the radiative effects of aerosols and clouds on the CO_2 fluxes for both sites was analyzed. Measurements of NEE, PARt, $\mathrm{PAR_f}$, AOD, relative humidity, air temperature and surface temperature of the forest canopy are further analyzed as a function of the relative irradiance parameter (f), during the biomass burning season at both sites.

3.1 MODIS AOD validation for the Central and Southwestern Amazon

The estimates of the MODIS AOD allowed to observe the atmospheric aerosol loadings from two geographic regions with very different characteristics. One region less impacted by anthropogenic activities (Manaus and Balbina), Central Amazon (Fig. 5a), and the other, heavily impacted by biomass burning smoke, represented by the site RBJ in Rondonia (Fig. 5c). Balbina (coordinates 1°55′1.14″ S and 59°29′12.48″ W) is a site close to K34, were AERONET measurements were done from 2000 to 2002. During the wet season, AOD values are small (around 0.10, a typical background value

for the Amazon), but increased significantly during the dry season with the long-range transport of biomass burning aerosol emissions. During the dry season, daily average AOD reached high values at RBJ (greater than 3.5) and at K34 (around 1.5) (Fig. 5a and c). These high atmospheric aerosol loadings from biomass burning cover very large areas of South America, and have impacts far from their source regions (Artaxo et al., 1998, 2002; Procopio et al., 2004; Martin et al., 2010a, b; Davidson et al., 2012).

Figure 5b and d shows that for both sites used in this study, MODIS and AERONET AOD agrees quite well, with values of R^2 that are statistically significant at the 95 % confidence level. In general, MODIS values tend to overestimate the AOD measurements at the two sites at 550 nm. The systematic errors (Mean Absolute Error – MAE) of the estimates with MODIS, show values around 5–10 % higher than AERONET measurements, are considered acceptable (Chu et al., 2002). The largest errors occur for AOD values greater than 1.0, where in some cases the MODIS values are higher than AERONET measurements by up to a factor of 2 (Fig. 5d). The regression analysis presented in Fig. 5b and d show that MODIS can be used to derive AOD, taking AERONET values as a reference. New validations could be implemented in future studies with the new MODIS high resolution 3 km aerosol product (Remer et al., 2013).

3.2 The influence of aerosols and clouds on PAR radiation and relative irradiance

In the present study, the impact of aerosols from biomass burning emissions on the radiation budget is assessed in terms of incident solar irradiance represented by the relative irradiance parameter f, PARt and PAR_f. The behavior of the relative irradiance f as a function of AOD, under minimal cloud effects is shown in Fig. 6a and 6b for K34 and RBJ respectively. In spite of the relatively large scattering, it is possible to observe a linear relationship, with relative irradiance reduced by 25 % for AOD values close to 0.5 at the K34 site. The linear relationship between f and AOD is significant statistically with p values < 0.01 with a R^2, ~ 0.22 (K34) and ~ 0.37 (RBJ). At $\cos(z)$ values for z between 10 and 35°, a reduction in the value of f on the order of 20 % was observed

when the AOD varied from 0.10 to 0.70 at the site of K34 (Fig. 6c) and approximately 25 % when the AOD varies from 0.10 to 2.5 in the forest area of RBJ.

Figure 6c and d shows the calculated fraction of diffuse radiation as a function of AOD. The calculation shows an increase of about 25 % in diffuse radiation as AOD increases from 0.2 to 0.60 (K34) and from 0.10 to 2.2 (RBJ). These results are particularly important because diffuse PAR penetrates more efficiently in the canopy and contributes to an increase in carbon uptake (Doughty et al., 2010). The joint analyses of Fig. 6 with the results shown in Sect. 3.5 helps to understand how the increase in AOD and PAR_f affect carbon uptake by the forest.

The Fig. 7a and b show that for f ranging from 0.80 to 1.2, the PARt is reduced by approximately 30–35 % at both sites K34 and RBJ. This behavior was observed both during the biomass burning season and the wet season. Oliveira et al. (2007) showed similar decreases ($\sim$ 20 %) when f varied from 1.0 to 0.80. These figures also show a strong reduction in PARt when the cloud cover changes from a "clear sky" conditions ($f > 1.0$, AOD ~ 0.10) to completely overcast by clouds and aerosols ($f < 1.0$, AOD $\gg$ 0.10). Although the PARt decreases almost linearly with the relative irradiance (Fig. 7a and b), the relationship between the diffuse PAR radiation and f is not linear (Fig. 7c and d). In this case, the PAR_f increases $\sim 500\,\mu mol\,m^{-2}\,s^{-1}$ when the relative irradiance f decreases from 1.2 to 0.75. This corresponds to a 50 % increase in PAR (diffuse) during biomass burning season due to scattering by aerosols and clouds. In the RBJ, these changes are mainly due to the dense aerosol layer observed during the biomass burning season.

3.3 The effect of PAR (diffuse) radiation on the light use efficiency (LUE) through forest

In Sects. 3.1 and 3.2, strong AOD seasonality was observed, with important effects in the atmospheric radiation balance, in particular, PAR radiation. In this section, the effect of these changes on the efficiency of radiation used by forests (LUE) was evaluated

and the values of radiation efficiency use for which this efficiency is maximum were identified.

Figure 8a and b shows NEE as a function of total PAR observed during clear-sky days and high aerosol loading/cloudy days during the dry season for both K34 and RBJ. The assimilation of carbon gradually increases with increasing total downward PAR (PARt) radiation reaching its maximum saturation at around 1800–2000 $\mu mol\,m^{-2}$ s for both sites (Fig. 8a and b). Additionally, it was observed that for the same level of irradiance at the surface (e.g., between 0–1800 $\mu mol\,m^{-2}\,s^{-1}$) the forest tends to absorb more carbon (more negative NEE) under high aerosol loading/cloudy atmospheric conditions (Fig. 8a and b). These results show that the fraction of diffuse solar radiation affects NEE at both sites in Amazonia.

Figure 8c and d shows the NEE normalized by the total PAR flux plotted against the diffuse fraction of PAR radiation. It is possible to analyze vegetation LUE analyzing the ratio of NEE/PAR-total (Jing et al., 2010). This relationship represents the photosynthetic efficiency, which is related to the ability of the canopy to convert solar energy into biomass. At both sites, it is possible to observe that LUE is low (~ 1–2 %), requiring large amounts of energy for photosynthesis. Furthermore, peaks of up to 4 % (K34) and 6 % (RBJ) in photosynthetic efficiency were observed in cases where the diffuse fraction reaches values around 1, during situations when the sky is obscured by clouds and aerosols ($f < 1.0$, AOD > 0.10). A gradual increase in LUE was observed (Fig. 8c and d) with increasing PAR (diffused) for irradiance values around 0.80, falling sharply after this value until the maximum fraction PAR_f which is 1.0. These results are similar to those obtained in the semiarid region of northeastern China (Jing et al., 2010).

3.4 Effect of aerosols and clouds on the Net Ecosystem Exchange (NEE)

Figure 9a and b shows the relationship between NEE and relative irradiance *f* for the experimental forest sites K34 and RBJ. In Fig. 9c and 9d the changes in net carbon absorbed by these forests (Relative Change of NEE, NEE %) due to aerosols (green dots) and clouds (black dots) can be observed. These analyses were performed with

the combined effect of clouds and aerosols. It is possible to observe at both sites that NEE has an inflection point at around $f \sim 0.8$. In other words, the maximum CO_2 fixation does not occur on a clear day ($f \sim 1.0$ and AOD < 0.10), but on days with either small cloud cover and/or moderate aerosol loading which increases the diffuse fraction of solar radiation. This effect was observed at both sites, during the dry season when there is a large loading of aerosols in the atmosphere and low cloud cover, and during the wet season, which experiences minimal aerosol content and frequent cloud cover (Figs. 5, 10b and 10c). However, this enhancement in NEE appears to occur from *f* values from 1.0 to ~ 0.8. For further reduction in the radiation field, the enhanced diffuse radiation does not compensate for the reduced total flux of solar radiation and the photosynthesis process is severally reduced (Fig. 9a and 9b). In short, diffuse radiation (PAR_f) increases the rate of photosynthesis only until a certain level of aerosol loading. A similar effect was also observed by Gu et al. (1999) and Doughty et al. (2010).

3.5 The net uptake of CO_2 due to aerosols and clouds

Through the use of Eqs. (1) and (8) it is possible to calculate the ratio of NEE (%) and the relative irradiance (*f*) for various intervals of zenithal angle. This procedure was adopted to minimize the effects of solar elevation throughout the day on NEE. For each SZA interval analyzed, the average NEE (%) for the clearness index *f* in bins equal to 0.1 (Fig. 9a, b) were calculated separately. At K34, an average increase of approximately 20 % in carbon uptake was observed relative to clear-sky (NEEcsky) conditions when the clearness index *f* is reduced from 1.1 to 0.8 (Fig. 9c). For this range of variation in *f*, AOD increases from 0.10 to 0.60 (Fig. 6a) and produces significant reductions in total PAR radiation flux (PARt), of approximately 50 % and, concomitantly, an increase of up to 25 % in PAR_f (Fig. 7c). At RBJ, the relative increase of NEE (%) was about 30 % when *f* varies from 1.1 to 0.80 (Fig. 9d). In the latter case, considering these same variations in *f*, the aerosol loading in the atmosphere increases AOD from 0.10 to 2.5 (Fig. 6b) producing reductions of up to 50 % of PAR and an increase of 25 % in PAR_f (Fig. 7d). The increase in carbon uptake in the presence of aerosols

and clouds becomes smaller and similar in both sites, for solar zenithal angles < 20° (Fig. 9c and d). Near zenith, solar radiation is less scattered by particles suspended in the atmosphere due to decreased path length, mitigating the diffuse radiation effects on the photosynthetic process.

The results from Fig. 9 shows that the photosynthetic efficiency of the forest is relatively larger on days with the atmosphere loaded with small amounts of aerosol particles and/or low cloud cover. The effect is clearly nonlinear, reaching a point where NEE begins to decrease. The value of this behavior varies for each solar zenith angle range. For measurements between 10–20°, a reduction in solar irradiance of up to 30 % does not inhibit CO_2 uptake in the forest canopy. For measurements taken for solar zenith angle between 20–35°, a 40 % reduction in irradiance does not show effects on CO_2 uptake. This result is important since much of the Amazon area is often impacted by the presence of aerosols in small amounts (low AOD) similar to those observed for Manaus. The increases in CO_2 uptake are significant and could have major impacts on the Amazon forest carbon budget. Peak CO_2 uptake is often observed for *f* values near 0.80, a value typically encountered in dense forest ecosystems (Gu et al., 1999; Yamasoe et al., 2006; Oliveira et al., 2007; Doughty et al., 2010) but quite different from what is found in grasslands and other temperate forested regions (Niyogi, 2004; Jing et al., 2010; Zhang et al., 2010).

3.6 The relationship between the current patterns of aerosols and clouds and carbon uptake

Figure 10 shows the percentage distribution of the kt (clearness index) throughout the year at K34 (1999–2009) and RBJ (1999–2002) sites. The percentage of cloud cover (not shown), as well as the distributions of kt (Fig. 10a and b) are similar for both sites, but differ from wet and dry seasons, as expected. Using brightness temperature from GOES10, 60 % of the time during the rainy season, both K34 and RBJ experienced some degree of cloud cover. This percentage, decreases during the dry season (August through October) reaching a minimum of 20 % at RBJ and 30 % at K34 in

September. The frequency distribution of kt (Fig. 10a and b), is compatible with the observations of cloud cover observed using GOES10 analysis (around 60–70 %).

The analysis of kt frequency distributions (Fig. 10a and b), indicates that current patterns of cloudiness do not yet exceed the maximum limit for which the forests of K34 and RBJ sites reach the maximum amounts of carbon uptake. The peak kt distribution at both sites is near 0.75 (Fig. 10b), which is smaller than the values of *f* for which the NEE reaches its maximum negative value during the burning season (kt ~ 0.57). This is the limit at which the cloudiness and/or aerosol load result in the maximum carbon uptake at RBJ and K34 (Fig. 10c). Larger quantities of aerosols and clouds in the region could cause these forests to absorb even greater amounts of carbon throughout the day, considering the combined effect of NEE enhancement by aerosols and clouds. The distribution patterns of the frequency occurrence of kt found throughout the years in both forest sites (Fig. 10) are similar to those found by Oliveira et al. (2007) in the Tapajos National Forest, in Santarem and Rondonia also in RBJ. These results are also consistent with calculations from Gu et al. (1999) in temperate forests of Canada, where kt values are centered at 0.75 and the maximum negative NEE is at about 0.55–0.60.

3.7 Effects of temperature and VPD on CO_2 uptake

Figure 11 shows the direct influence that clouds and aerosols have on some of the major environmental factors that also affect the photosynthetic activity of plants. The attenuation of incident solar irradiance due to the presence of aerosols and clouds, cause significant reductions in air temperature near the canopy forest and also in the vapor pressure deficit (VPD) associated with relative humidity (Fig. 11). At the K34 site, the combined effect of aerosols and clouds (in this case, more aerosols than clouds) produced, respectively, a cooling of 1.5 and 2.5 °C in air temperature of the canopy when *f* ranged from 1.2 to 0.80 (Fig. 11a and c). At RBJ, considering the same variations in *f*, a cooling of 3–4 °C was observed (Fig. 11b and d). These values are on the relatively high side, but are similar to results found by Davidi et al. (2009). Another

factor that can increase canopy photosynthesis is the general trend of decreasing vapor pressure deficit on cloudy or smoke-filled skies (Min and Wang, 2005, 2008; Bai, et al., 2012). Figure 11e and f shows the relationship between the VPD and irradiance on *f* (again, between solar zenithal angle 10–35°). For Freedman et al. (1998), increasing relative humidity due to cloud/aerosol-induced cooling (Altaratz et al., 2008), can increase photosynthesis since this increase naturally induces the opening of the stomata of the leaves (Collatz et al., 1991). At both sites, the reduction in *f* produced an increase in VPD of up to 15 % during the dry season. The reductions observed in the vapor pressure deficit associated with reductions in air temperature in the forest canopy can also be contributing to an increase in NEE.

4 Conclusions

Aerosol optical depth derived by MODIS has been shown to be satisfactory for two different sites in the Amazon, after comparisons with AERONET AOD. This allows the expansion of studies of aerosol effects on the Amazonian ecosystem to other areas of the Amazon, where no AERONET measurements exist. Given the long time series of micrometeorological measurements at the K34 and RBJ sites, it was possible to assess the reduction in solar irradiance due to the presence of clouds and aerosols emitted by biomass burning. The clear-sky irradiance algorithm developed was able to satisfactorily quantity the reduction in surface radiation flux, taking into account an atmosphere free of clouds and with minimal aerosol loading. Thus, the changes in incident solar radiation and CO_2 flux (NEE) could be attributed to the combined effect of clouds and aerosol. In Central Amazonia (K34 site), the net carbon flux (NEE) increased by 20 % when the optical depth ranged from 0.10 to 0.65. At the RBJ site, a stronger effect was observed, with an increase of 29 % on the NEE observed when AOD varied between 0.1 and 2. Aerosols from biomass burning produced up to a 50 % reduction in the amount of total incident solar radiation and also an increase of up to 25 % in the fraction of diffuse solar radiation, which is utilized more efficiently by the

forest photosynthesis process. The results show higher photosynthetic efficiency in situations where the atmosphere is lightly loaded with particles and/or clouds. A more efficient use of the diffuse solar radiation can be pointed to as the main source of increased CO_2 flux in the forest areas of the sites studied. In addition, in view of the increased cloudiness and aerosol loading, significant variations were observed in other meteorological variables, such as temperature and vapor pressure deficit (VPD). The variations of these quantities may also influence carbon uptake.

The increase in VPD associated with decreased air temperature due to aerosols and clouds may be causing reductions in the rate of respiration of forest and hence an increase in NEE, during biomass burning aerosols exposure. Many physiological and environmental factors also are involved in the dynamics and control of carbon fluxes in the Amazon, thereby attributing and separating the different effects on CO_2 fluxes difficult.

The increase in NEE due to the increased amount of aerosols and clouds constitute an effect of considerable relevance due to the importance of carbon cycling in Amazonia. A regional study of this effect, based on vegetation maps, remote sensing estimates, assimilated meteorological data and environmental modeling, will help to better understand how climate and ecosystem functioning in Amazonia are affected by natural and anthropogenic environmental factors.

Acknowledgements. We thank FAPESP projects 2008/58100-2 (AEROCLIMA), 2010/52658-1 and 2011/50170-4 for financial support. We also thank financial support from CAPES and CNPq thought the projects 477575/2008-, 475735/2012-9 and the Brazilian National Institute of Science and Technology (INCT) for Climate Change funded by CNPq Grant Number 573797/2008-0 and FAPESP Grant Number 2008/57719-9. We acknowledge the Instituto Nacional de Pesquisas da Amazônia INPA/CLIAMB and the INPA/LBA Central Office for logistical support. We thank several key persons for the support on aerosol sampling and analysis: Alcides C. Ribeiro, Ana Lucia Loureiro, Fernando G. Morais and Fábio O. Jorge. Thanks go to Luiz Machado, Roberto Freitas (INPE/DSA, Brazil) and Alexandre L. Correia (IF /USP) for GOES data and MODIS data.

References

Abakumova, G. M., Feigelson, E. M., Russak, V., and Stadnik, V. V.: Evaluation of long-term changes in radiation, cloudiness, and surface temperature on the territory of the former soviet union, J. Climate, 9, 1319–1327, 1996.

Adams, D. K., Fernandes, R. M. S., and Maia, J. M. F.: GNSS precipitable water vapor from an Amazonian rain forest flux tower, J. Atmos. Ocean. Tech., 28, 1192–1198, doi:10.1175/Jtech-D-11-00082.1, 2011.

Altaratz, O., Koren, I., and Reisin, T.: Humidity impact on the aerosol effect in warm cumulus clouds, Geophys. Res. Lett., 35, L17804, doi:10.1029/2008gl034178, 2008.

Andreae, M. O., Rosenfeld, D., Artaxo, P., Costa, A. A., Frank, G. P., Longo, K. M., and Silva-Dias, M. A. F.: Smoking rain clouds over the Amazon, Science, 303, 1337–1342, doi:10.1126/science.1092779, 2004.

Araujo, A. C., Nobre, A. D., Kruijt, B., Elbers, J. A., Dallarosa, R., Stefani, P., von Randow, C., Manzi, A. O., Culf, A. D., Gash, J. H. C., Valentini, R., and Kabat, P.: Comparative measurements of carbon dioxide fluxes from two nearby towers in a central Amazonian rainforest: the Manaus LBA site, J. Geophys. Res.-Atmos., 107, 8090, doi:10.1029/2001jd000676, 2002.

Artaxo, P., Fernandes, E. T., Martins, J. V., Yamasoe, M. A., Hobbs, P. V., Maenhaut, W., Longo, K. M., and Castanho, A.: Large-scale aerosol source apportionment in Amazonia, J. Geophys. Res.-Atmos., 103, 31837–31847, doi:10.1029/98jd02346, 1998.

Artaxo, P., Martins, J. V., Yamasoe, M. A., Procopio, A. S., Pauliquevis, T. M., Andreae, M. O., Guyon, P., Gatti, L. V., and Leal, A. M. C.: Physical and chemical properties of aerosols in the wet and dry seasons in Rondonia, Amazonia, J. Geophys. Res.-Atmos., 107, 8081, doi:10.1029/2001jd000666, 2002.

Artaxo, P., Rizzo, L. V., Paixao, M., de Lucca, S., Oliveira, P. H., Lara, L. L., Wiedemann, K. T., Andreae, M. O., Holben, B., Schafer, J., Correia, A. L., and Pauliquevis, T. M.: Aerosol particles in Amazonia: their composition, role in the radiation balance, cloud formation, and nutrient cycles, Geophys. Monogr. Ser., 186, 233–250, doi:10.1029/2008gm000778, 2009.

Artaxo, P., Rizzo, L. V., Brito, J. F., Barbosa, H. M. J., Arana, A., Sena, E. T., Cirino, G. G., Bastos, W., Martin, S. T., and Andreae, M. O.: Atmospheric aerosols in Amazonia and land use change: from natural biogenic to biomass burning conditions, Faraday Discuss., doi:10.1039/C3FD00052D, 2013.

Aubinet, M., Grelle, A., Ibrom, A., Rannik, U., Moncrieff, J., Foken, T., Kowalski, A. S., Martin, P. H., Berbigier, P., Bernhofer, C., Clement, R., Elbers, J., Granier, A., Grunwald, T., Morgenstern, K., Pilegaard, K., Rebmann, C., Snijders, W., Valentini, R., and Vesala, T.: Estimates of the annual net carbon and water exchange of forests: the EUROFLUX methodology, Adv. Ecol. Res., 30, 113–175, 2000.

Aubinet, M., Chermanne, B., Vandenhaute, M., Longdoz, B., Yernaux, M., and Laitat, E.: Long term carbon dioxide exchange above a mixed forest in the Belgian Ardennes, Agr. Forest Meteorol., 108, 293–315, doi:10.1016/S0168-1923(01)00244-1, 2001.

Bai, Y., Wang, J., Zhang, B., Zhang, Z., and Liang, J.: Comparing the impact of cloudiness on carbon dioxide exchange in a grassland and a maize cropland in northwestern China, Ecol. Res., 27, 615–623, doi:10.1007/s11284-012-0930-z, 2012.

Baldocchi, D.: Measuring and modelling carbon dioxide and water vapour exchange over a temperate broad-leaved forest during the 1995 summer drought, Plant Cell Environ., 20, 1108–1122, doi:10.1046/j.1365-3040.1997.d01-147.x, 1997.

Benner, T. C. and Curry, J. A.: Characteristics of small tropical cumulus clouds and their impact on the environment, J. Geophys. Res.-Atmos., 103, 28753–28767, doi:10.1029/98jd02579, 1998.

Betts, A. K. and Dias, M. A. F. S.: Progress in understanding land–surface–atmosphere coupling from LBA research, J. Adv. Model Earth Syst., doi:10.3894/James.2010.2.6, 2010.

Collatz, G. J., Ball, J. T., Grivet, C., and Berry, J. A.: Physiological and environmental-regulation of stomatal conductance, photosynthesis and transpiration – a model that includes a laminar boundary-layer, Agr. Forest Meteorol., 54, 107–136, doi:10.1016/0168-1923(91)90002-8, 1991.

Chu, D. A., Kaufman, Y. J., Ichoku, C., Remer, L. A., Tanré, D., and Holben, B. N.: Validation of MODIS aerosol optical depth retrieval over land, Geophys. Res. Lett., 29, 8007, doi:10.1029/2001GL013205, 2002.

da Rocha, H. R., Goulden, M. L., Miller, S. D., Menton, M. C., Pinto, L. D. V. O., de Freitas, H. C., and Figueira, A. M. E. S.: Seasonality of water and heat fluxes over a tropical forest in eastern Amazonia, Ecol. Appl., 14, 22–32, 2004.

da Rocha, H. R., Manzi, A. O., Cabral, O. M., Miller, S. D., Goulden, M. L., Saleska, S. R., Coupe, N. R., Wofsy, S. C., Borma, L. S., Artaxo, P., Vourlitis, G., Nogueira, J. S., Cardoso, F. L., Nobre, A. D., Kruijt, B., Freitas, H. C., von Randow, C., Aguiar, R. G., and Maia, J. F.: Patterns of water and heat flux across a biome gradient from tropical forest

to savanna in Brazil, J. Geophys. Res.-Biogeo., 114, G00b12, doi:10.1029/2007jg000640, 2009.

Davidi, A., Koren, I., and Remer, L.: Direct measurements of the effect of biomass burning over the Amazon on the atmospheric temperature profile, Atmos. Chem. Phys., 9, 8211–8221, doi:10.5194/acp-9-8211-2009, 2009.

Davidson, E. A., de Araujo, A. C., Artaxo, P., Balch, J. K., Brown, I. F., Bustamante, M. M. C., Coe, M. T., DeFries, R. S., Keller, M., Longo, M., Munger, J. W., Schroeder, W., Soares, B. S., Souza, C. M., and Wofsy, S. C.: The Amazon basin in transition, Nature, 481, 321–328, doi:10.1038/Nature10717, 2012.

de Araujo, A. C., Dolman, A. J., Waterloo, M. J., Gash, J. H. C., Kruijt, B., Zanchi, F. B., de Lange, J. M. E., Stoevelaar, R., Manzi, A. O., Nobre, A. D., Lootens, R. N., and Backer, J.: The spatial variability of CO2 storage and the interpretation of eddy covariance fluxes in central Amazonia, Agr. Forest Meteorol., 150, 226–237, 2010.

Dolman, A. J., Valentini, R., Groenendijk, M., and Hendriks, D.: Flux tower sites, state of the art, and network design, in: The Continental-Scale Greenhouse Gas Balance of Europe, edited by: Dolman, A. J., Valentini, R., and Freibauer, A., Ecological Studies, Springer, New York, 215–242, 2008.

Doughty, C. E., Flanner, M. G., and Goulden, M. L.: Effect of smoke on subcanopy shaded light, canopy temperature, and carbon dioxide uptake in an Amazon rainforest, Global Biogeochem. Cy., 24, GB3015, doi:10.1029/2009gb003670, 2010.

Duchon, C. E. and O'Malley, M. S.: Estimating cloud type from pyranometer observations, J. Appl. Meteorol., 38, 132–141, 1999.

Eck, T. F., Holben, B. N., Reid, J. S., O'Neill, N. T., Schafer, J. S., Dubovik, O., Smirnov, A., Yamasoe, M. A., and Artaxo, P.: High aerosol optical depth biomass burning events: a comparison of optical properties for different source regions, Geophys. Res. Lett., 30, 2035, doi:10.1029/2003gl017861, 2003.

Ferraz, J., Ohta, S., and Salles, P. C.: Distribuição dos solos ao longo de dois transectos em floresta primária ao norte de Manaus (AM), in: Pesquisas Florestais para Conservação da Floresta e Reabilitação de Áreas Degradadas da Amazônia, Manaus-AM, Brazil, MCT-INPA/JICAm, edited by: Higuchi, N., Campos, M. A. A., Sampaio, P. T. B., Santos, J., 111–143, 1998.

Finnigan, J.: The storage term in eddy flux calculations, Agr. Forest Meteorol., 136, 108–113, doi:10.1016/j.agrformet.2004.12.010, 2006.

Fisch, G., Marengo, J. A., and Nobre, C.: The climate of Amazonia – a review, Acta Amazonica, 28, 101–126, 1998 (in Portugese).

Freedman, J. M., Fitzjarrald, D. R., Moore, K. E., and Sakai, R. K.: Boundary layer cloud climatology and enhanced forest-atmosphere exchange, in: Preprints of 23rd Conference on Agricultural and Forest Meteorology, American Meteorology Society, Boston, Mass., 41–44, 1998.

Gates, D. M.: Biophysical Ecology, Springer, New York, 611 pp., 1980.

Goulden, M. L., Daube, B. C., Fan, S. M., Sutton, D. J., Bazzaz, A., Munger, J. W., and Wofsy, S. C.: Physiological responses of a black spruce forest to weather, J. Geophys. Res.-Atmos., 102, 28987–28996, doi:10.1029/97jd01111, 1997.

Gu, L., Fuentes, J. D., Shugart, H. H., Staebler, R. M., and Black, T. A.: Responses of net ecosystem exchanges of carbon dioxide to changes in cloudiness: results from two North American deciduous forests, J. Geophys. Res.-Atmos, 104, 31421–31434, doi:10.1029/1999jd901068, 1999.

Gu, L., Fuentes, J. D., Garstang, M., Silva, J. T. D., Heitz, R., Sigler, J., and Shugart, H. H.: Cloud modulation of surface solar irradiance at a pasture site in southern Brazil, Agr. Forest Meteorol., 106, 117–129, 2001.

Gu, L. H., Baldocchi, D. D., Wofsy, S. C., Munger, J. W., Michalsky, J. J., Urbanski, S. P., and Boden, T. A.: Response of a deciduous forest to the Mount Pinatubo eruption: enhanced photosynthesis, Science, 299, 2035–2038, doi:10.1126/science.1078366, 2003.

Guyon, P., Graham, B., Beck, J., Boucher, O., Gerasopoulos, E., Mayol-Bracero, O. L., Roberts, G. C., Artaxo, P., and Andreae, M. O.: Physical properties and concentration of aerosol particles over the Amazon tropical forest during background and biomass burning conditions, Atmos. Chem. Phys., 3, 951–967, doi:10.5194/acp-3-951-2003, 2003.

Higuchi, N., dos Santos, J., Vieira, G., Ribeiro, R. J., Sakurai, S., Ishizuka, M., Sakai, T., Tanaka, N., and Saito, S.: Análise estrutural da floresta primária da bacia do rio Cuieiras, ZF-2, Manaus-AM, Brasil, in: Pesquisas florestais para a conservação da floresta e reabilitação de áreas degradadas da Amazônia, edited by: Higuchi, N. A., Campos, M. A. A., Sampaio, P. T. B., and dos Santos, J., MCT-INPA/JICA, Manaus, 51–91, 1998.

Holben, B. N., Setzer, A., Eck, T. F., Pereira, A., and Slutsker, I.: Effect of dry-season biomass burning on Amazon basin aerosol concentrations and optical properties, 1992–1994, J. Geophys. Res.-Atmos., 101, 19465–19481, doi:10.1029/96jd01114, 1996.

Holben, B. N., Eck, T. F., Slutsker, I., Tanre, D., Buis, J. P., Setzer, A., Vermote, E., Reagan, J. A., Kaufman, Y. J., Nakajima, T., Lavenu, F., Jankowiak, I., and Smirnov, A.: AERONET – a federated instrument network and data archive for aerosol characterization, Remote Sens. Environ., 66, 1–16, doi:10.1016/S0034-4257(98)00031-5, 1998.

Houghton, R. A., Skole, D. L., Nobre, C. A., Hackler, J. L., Lawrence, K. T., and Chomentowski, W. H.: Annual fluxes or carbon from deforestation and regrowth in the Brazilian Amazon, Nature, 403, 301–304, doi:10.1038/35002062, 2000.

Hutyra, L. R., Munger, J. W., Hammond-Pyle, E., Saleska, S. R., Restrepo-Coupe, N., Daube, B. C., de Camargo, P. B., and Wofsy, S. C.: Resolving systematic errors in estimates of net ecosystem exchange of CO_2 and ecosystem respiration in a tropical forest biome, Agr. Forest Meteorol., 148, 1266–1279, doi:10.1016/j.agrformet.2008.03.007, 2008.

Jing, X., Huang, J., Wang, G., Higuchi, K., Bi, J., Sun, Y., Yu, H., and Wang, T.: The effects of clouds and aerosols on net ecosystem CO_2 exchange over semi-arid Loess Plateau of Northwest China, Atmos. Chem. Phys., 10, 8205–8218, doi:10.5194/acp-10-8205-2010, 2010.

Keeling, C. D., Chin, J. F. S., and Whorf, T. P.: Increased activity of northern vegetation inferred from atmospheric CO_2 measurements, Nature, 382, 146–149, 1996.

Keller, M., Clark, D. A., Clark, D. B., Weitz, A. M., and Veldkamp, E.: If a tree falls in the forest. . . , Science, 273, 5272, doi:10.1126/science.273.5272.201, 1996.

King, M. D., Kaufman, Y. J., Tanre, D., and Nakajima, T.: Remote sensing of tropospheric aerosols from space: past, present, and future, B. Am. Meteorol. Soc., 80, 2229–2259, 1999.

King, M. D., Menzel, W. P., Kaufman, Y. J., Tanre, D., Gao, B. C., Platnick, S., Ackerman, S. A., Remer, L. A., Pincus, R., and Hubanks, P. A.: Cloud and aerosol properties, precipitable water, and profiles of temperature and water vapor from MODIS, IEEE T. Geosci. Remote, 41, 442–458, doi:10.1109/Tgrs.2002.808226, 2003.

Law, B. E., Falge, E., Gu, L., Baldocchi, D. D., Bakwin, P., Berbigier, P., Davis, K., Dolman, A. J., Falk, M., Fuentes, J. D., Goldstein, A., Granier, A., Grelle, A., Hollinger, D., Janssens, I. A., Jarvis, P., Jensen, N. O., Katul, G., Mahli, Y., Matteucci, G., Meyers, T., Monson, R., Munger, W., Oechel, W., Olson, R., Pilegaard, K., Paw, K. T., Thorgeirsson, H., Valentini, R., Verma, S., Vesala, T., Wilson, K., and Wofsy, S.: Environmental controls over carbon dioxide and water vapor exchange of terrestrial vegetation, Agr. Forest Meteorol., 113, 97–120, doi:10.1016/S0168-1923(02)00104-1, 2002.

Loescher, H. W., Law, B. E., Mahrt, L., Hollinger, D. Y., Campbell, J., and Wofsy, S. C.: Uncertainties in, and interpretation of, carbon flux estimates using the eddy covariance technique, J. Geophys. Res.-Atmos., 111, D21S90, doi:10.1029/2005jd006932, 2006.

Machado, L. A. T., Laurent, H., Dessay, N., and Miranda, I.: Seasonal and diurnal variability of convection over the Amazonia: a comparison of different vegetation types and large scale forcing, Theor. Appl. Climatol., 78, 61–77, 2004.

Mahrt, L.: Computing turbulent fluxes near the surface: needed improvements, Agr. Forest Meteorol., 150, 501–509, doi:10.1016/j.agrformet.2010.01.015, 2010.

Malhi, Y.: The carbon balance of tropical forest regions, 1990–2005, Curr. Opin. Sust., 2, 237–244, doi:10.1016/j.cosust.2010.08.002, 2010.

Malhi, Y.: The productivity, metabolism and carbon cycle of tropical forest vegetation, J. Ecol., 100, 65–75, doi:10.1111/j.1365-2745.2011.01916.x, 2012.

Martin, S. T., Andreae, M. O., Artaxo, P., Baumgardner, D., Chen, Q., Goldstein, A. H., Guenther, A., Heald, C. L., Mayol-Bracero, O. L., McMurry, P. H., Pauliquevis, T., Poschl, U., Prather, K. A., Roberts, G. C., Saleska, S. R., Dias, M. A. S., Spracklen, D. V., Swietlicki, E., and Trebs, I.: Sources and properties of Amazonian aerosol particles, Rev. Geophys., 48, RG2002, doi:10.1029/2008rg000280, 2010a.

Martin, S. T., Andreae, M. O., Althausen, D., Artaxo, P., Baars, H., Borrmann, S., Chen, Q., Farmer, D. K., Guenther, A., Gunthe, S. S., Jimenez, J. L., Karl, T., Longo, K., Manzi, A., Müller, T., Pauliquevis, T., Petters, M. D., Prenni, A. J., Pöschl, U., Rizzo, L. V., Schneider, J., Smith, J. N., Swietlicki, E., Tota, J., Wang, J., Wiedensohler, A., and Zorn, S. R.: An overview of the Amazonian Aerosol Characterization Experiment 2008 (AMAZE-08), Atmos. Chem. Phys., 10, 11415–11438, doi:10.5194/acp-10-11415-2010, 2010.

Mercado, L. M., Bellouin, N., Sitch, S., Boucher, O., Huntingford, C., Wild, M., and Cox, P. M.: Impact of changes in diffuse radiation on the global land carbon sink, Nature, 458, 1014–1087, doi:10.1038/Nature07949, 2009.

Miller, S. D., Goulden, M. L., Menton, M. C., da Rocha, H. R., de Freitas, H. C., Figueira, A. M. E. S., and de Sousa, C. A. D.: Biometric and micrometeorological measurements of tropical forest carbon balance, Ecol. Appl., 14, 114–126, 2004.

Min, Q.: Impacts of aerosols and clouds on forest-atmosphere carbon exchange, J. Geophys. Res.-Atmos., 35, L02406, doi:10.1029/2007GL032398, 2005.

Min, Q. and Wang, S.: Clouds modulate terrestrial carbon uptake in a midlatitude hardwood forest, Geophys. Res. Lett., 35, L02406, doi:10.1029/2007GL032398, 2008.

Moncrieff, J. B., Massheder, J. M., De Bruin, H., Elbers, J., Friborg, T., Heusinkveld, B., Kabat, P., Scott, S., Soegaard, H., and Verhoef, A.: A system to measure surface fluxes of momentum, sensible heat, water vapour and carbon dioxide, J. Hydrol., 188–189, 589–611, 1997.

Monteith, J. L. and Unsworth, M. H.: Principles of Environmental Physics, Edward Arnold, London, UK, 1990.

Myneni, R. B., Keeling, C. D., Tucker, C. J., Asrar, G., and Nemani, R. R.: Increased plant growth in the northern high latitudes from 1981 to 1991, Nature, 386, 698–702, doi:10.1038/386698a0, 1997.

Niyogi, D., Chang,H.-I., Saxena, V. K., Holt, T., Alapaty, K., Booker, F., Chen, F., Davis, K. J., Holben, B., Matsui, T., Meyers, T., Oechel, W. C., Pielke Sr., R. A., Wells, R., Wilson, K., and Xue, Y.: Direct observations of the effects of aerosol loading on net ecosystem CO_2 exchanges over different landscapes, Geophys. Res. Lett., 31, L20506, doi:10.1029/2004gl020915, 2004.

Oliveira, A. N. D. and Amaral, I. L. D.: Floristic, phytosociological and ecological aspects of terra firme understory in central Amazonia, Amazonas state, Brazil, Acta Amazonica, 35, 1–16, 2005 (in Portugese).

Oliveira, P. H. F., Artaxo, P., Pires, C., De Lucca, S., Procópio, A., Holben, B., Schafer, J., Cardoso, L. F., Wofsy, S. C., and Rocha, H. R.: The effects of biomass burning aerosols and clouds on the CO_2 flux in Amazonia, Tellus B, 59, 338–349, doi:10.1111/j.1600-0889.2007.00270.x, 2007.

Ometto, J. P., Nobre, A. D., Rocha, H. R., Artaxo, P., and Martinelli, L. A.: Amazonia and the modern carbon cycle: lessons learned, Oecologia, 143, 483–500, doi:10.1007/s00442-005-0034-3, 2005.

Phillips, O. L., Malhi, Y., Higuchi, N., Laurance, W. F., Núñez, P. V., Vásquez, R. M., Laurance, S. G., Ferreira, L. V., Stern, M., Brown, S., and Grace, J.: Changes in the carbon balance of tropical forests: evidence from long-term plots, Science, 282, 439–442, doi:10.1126/science.282.5388.439, 1998.

Procopio, A. S., Artaxo, P., Kaufman, Y. J., Remer, L. A., Schafer, J. S., and Holben, B. N.: Multiyear analysis of amazonian biomass burning smoke radiative forcing of climate, Geophys. Res. Lett., 31, L03108, doi:10.1029/2003gl018646, 2004.

Reindl, D. T., Beckman, W. A., and Duffie, J. A.: Diffuse fraction correlations, Sol. Energy, 45, 1–7, doi:10.1016/0038-092x(90)90060-P, 1990.

Remer, L. A., Kaufman, Y. J., Tanre, D., Mattoo, S., Chu, D. A., Martins, J. V., Li, R. R., Ichoku, C., Levy, R. C., Kleidman, R. G., Eck, T. F., Vermote, E., and Holben, B. N.: The MODIS aerosol algorithm, products, and validation, J. Atmos. Sci., 62, 947–973, doi:10.1175/Jas3385.1, 2005.

Remer, L. A., Mattoo, S., Levy, R. C., and Munchak, L. A.: MODIS 3 km aerosol product: algorithm and global perspective, Atmos. Meas. Tech., 6, 1829–1844, doi:10.5194/amt-6-1829-2013, 2013.

Rennó, C. D., Nobre, A. D., Cuartas, L. A., Soares, J. V., Hodnett, M. G., Tomasella, J., and Waterloo, M. J.: HAND, a new terrain descriptor using SRTM-DEM: mapping terra-firme rainforest environments in Amazonia, Remote Sens. Environ., 112, 3469–3481, 2008.

Ricchiazzi, P., Yang, S., Gautier, C., and Sowle, D.: SBDART: a research and teaching software tool for plane-parallel radiative transfer in the Earth's atmosphere, B. Am. Meteorol. Soc., 79, 2101–2114, 1998.

Richardson, A. D. and Hollinger, D. Y.: Statistical modeling of ecosystem respiration using eddy covariance data: Maximum likelihood parameter estimation, and Monte Carlo simulation of model and parameter uncertainty, applied to three simple models, Agr. Forest Meteorol., 131, 191–208, doi:10.1016/j.agrformet.2005.05.008, 2005.

Schafer, J. S., Eck, T. F., Holben, B. N., Artaxo, P., Yamasoe, M. A., and Procopio, A. S.: Observed reductions of total solar irradiance by biomass-burning aerosols in the Brazilian Amazon and Zambian Savanna, Geophys. Res. Lett., 29, 1823, doi:10.1029/2001gl014309, 2002.

Seinfeld, J. H. and Pandis, S. N.: Atmospheric Chemistry and Physics – from Air Pollution to Climate Change, 2nd edn., John Wiley & Sons, USA, 2006.

Sena, E. T., Artaxo, P., and Correia, A. L.: Spatial variability of the direct radiative forcing of biomass burning aerosols and the effects of land use change in Amazonia, Atmos. Chem. Phys., 13, 1261–1275, doi:10.5194/acp-13-1261-2013, 2013.

Silva Dias, M. A. F., Rutledge, S., Kabat, P., Silva Dias, P. L., Nobre, C., Fisch, G., Dolman, A. J., Zipser, E., Garstang, M., Manzi, A. O., Fuentes, J. D., Rocha, H. R., Marengo, J., Plana-Fattori, A., Sá, L. D. A., Alvalá, R. C. S., Andreae, M. O., Artaxo, P., Gielow, R., and Gatti, L.: Cloud and rain processes in a biosphere–atmosphere interaction context in the Amazon Region, J. Geophys. Res.-Atmos., 107, 8072, doi:10.1029/2001jd000335, 2002.

Spitters, C. J. T.: Separating the diffuse and direct component of global radiation and its implications for modeling canopy photosynthesis .2. Calculation of canopy photosynthesis, Agr. Forest Meteorol., 38, 231–242, doi:10.1016/0168-1923(86)90061-4, 1986.

Tóta, J., Fitzjarrald, D. R., Staebler, R. M., Sakai, R. K., Moraes, O. M. M., Acevedo, O. C., Wofsy, S. C., and Manzi, A. O.: Amazon rain forest subcanopy flow and the carbon budget: Santarém LBA-ECO site, J. Geophys. Res., 113, G00B02, doi:10.1029/2007jg000597, 2008.

von Randow, C., Manzi, A. O., Kruijt, B., de Oliveira, P. J., Zanchi, F. B., Silva, R. L., Hodnett, M. G., Gash, J. H. C., Elbers, J. A., Waterloo, M. J., Cardoso, F. L., and Kabat, P.: Comparative measurements and seasonal variations in energy and carbon exchange over forest and pasture in South West Amazonia, Theor. Appl. Climatol., 78, doi:10.1007/s00704-004-0041-z, 2004.

Vourlitis, G. L., de Almeida Lobo, F., Zeilhofer, P., and de Souza Nogueira, J.: Temporal patterns of net CO_2 exchange for a tropical semideciduous forest of the southern Amazon Basin, J. Geophys. Res., 116, G03029, doi:10.1029/2010jg001524, 2011.

Yamasoe, M. A., von Randow, C., Manzi, A. O., Schafer, J. S., Eck, T. F., and Holben, B. N.: Effect of smoke and clouds on the transmissivity of photosynthetically active radiation inside the canopy, Atmos. Chem. Phys., 6, 1645–1656, doi:10.5194/acp-6-1645-2006, 2006.

Zhang, M., Yu, G.-R., Zhang, L.-M., Sun, X.-M., Wen, X.-F., Han, S.-J., and Yan, J.-H.: Impact of cloudiness on net ecosystem exchange of carbon dioxide in different types of forest ecosystems in China, Biogeosciences, 7, 711–722, doi:10.5194/bg-7-711-2010, 2010.

Table 1. List of measurements, instruments and measurement heights for the automatic weather station and eddy correlation instrumentation installed on the K34/Manaus-AM and RBJ/Ji-Paraná LBA towers.

Set list instruments and measurements				
Measurements	Instruments	[Unit]	Measurements height [m]	
			K34	RBJ
Net Radiation	NR-LITE Kipp & Zonen	$W m^{-2}$	44.0	19.0
Incident and reflected short wave radiation	Pyranometers Kipp & Zonen (CM21)	$W m^{-2}$	44.6	19.3[a]
Incident and emitted long wave radiation	Pyrgeometers Kipp & Zonen (CG1)	$W m^{-2}$	44.6	19.3[a]
Photosynthetically Active Radiation (PAR)	LI-COR LI-190SZ quantum sensor	$\mu mol\, m^{-2} s^{-1}$	51.6	25.6[a]
Vertical profile of air temperature	Vaisala thermohygrometer (HMP35A)/PT100 resistors	°C	51.1, 42.5, 35.5, 28.0, 15.6, 5.2	60.0, 45.2, 35.0, 25.3, 15.3, 5.3
Vertical profile of [CO_2] and water vapour [H_2O]	IRGA PP Systems CIRAS SC	ppm	51.1, 42.5, 35.5, 28.0, 15.6, 5.2	62.7, 45.0, 35.0, 25.0, 2.7, 0.05
Relative Humidty	Vaisala thermohygrometer (HMP35A) and (HMP45AC)/PT100 resistors	%	51.1	60.0
Rainfall	Rain gauge EM ARG-100	mm	51.3	60.3
Atmospheric pressure	Barometer Vaisala (PTB100A)	hPa (mb)	32.0	40.0
u, v, w (wind vector)	Eddy correlation system (Gill Sonic Anemometer and LI-COR 6262 IRGA)	$m s^{-1}$	53.1 and 46.1	62.7

[a]Height above canopy top (~ 35 m)

Table 2. Average values of net ecosystem exchange measured over the two sites during daytime (08:30–17:30 h) and nighttime (19:00–05:00 h), for wet and dry seasons. Also included are the peak photosynthesis activity and daily totals.

	Wet Season $\mu mol\,m^{-2}\,s^{-1}$				Dry Season $\mu mol\,m^{-2}\,s^{-1}$			
Rainfall Forest	Daytime	Nighttime	Day peak	Daily Total[a]	Daytime	Nighttime	Day peak	Daily total[a]
K34 [1999–2009]	−10.2	4.2	−25.1	−19.9	−9.3	3.0	−24.0	−23.8
RBJ [1999–2002]	−15.1	8.1	−35.1	−24.1	−11.2	6.6	−31.8	−14.6
Ecosytem change effect								
$\lvert F_{RBJ}\rvert - \lvert F_{K34}\rvert$	4.9	3.9	10.0	4.2	1.9	3.6	7.8	−9.2
$[\lvert F_{RBJ}\rvert - \lvert F_{K34}\rvert]/\lvert F_{K34}\rvert$[b]	48.0[b]	92.9	39.8[b]	21.1[b]	20.4[b]	123.4	32.5[b]	−38.7[b]

[a] Daily totals of absorbed carbon $kg\,C\,ha^{-1}\,day^{-1}$.
[b] Note that this percent (%) increase and decrease is related to negative values (uptake by photosynthesis).

Table 3. Regression coefficients of relationships between clear-sky irradiance (S_0) and solar zenithal angles cos(z) as well as relationships between clear-sky clearness index (kt^*) and solar zenithal angles cos(z) of Eq. (7) for the morning and afternoon periods of the K34 and RBJ sites. Periods of measurements: K34: 2000–2009, and RBJ: 2000–2002.

Regression Coef.	Trop. Rainforest Manaus (K34) Morning	Afternoon	Trop. Rainforest Ji-Parana (RBJ) Morning	Afternoon
Clear-sky irradiance $[S_0] - [S_0' = p_1\cos^3(z) + p_2\cos^2(z) + p_3\cos(z) + p_4]$				
p_1	−1026	−685	−813	−644
p_2	2027	1210	1867	1188
p_3	−110	240	−170	295
p_4	10	14	11	18
R^2	0.95	0.85	0.95	0.92
Clear-sky clearness index $[kt^*] - [kt_0 = a_1\cos^3(z) + a_2\cos^2(z) + a_3\cos(z) + a_4]$				
a_1	−0.01	−0.31	−0.14	−0.54
a_2	−0.69	0.16	−0.29	0.63
a_3	1.39	0.41	1.13	0.13
a_4	−0.02	0.31	−0.04	0.41
R^2	0.85	0.30	0.87	0.41

Table 4. Regression coefficients of relationship between NEE and solar zenithal angle (SZA) for clear-sky conditions ($f \sim 1.0$) observed during the dry seasons at the K34 and RBJ sites.

Measurements (morning) Clear-sky	Regression of Parameters n_1^*	n_2^*	n_3^*	R^2
Trop. Rainforest (RBJ)/2000–2002				
NEE of CO_2 – µmol m^{-1} s^{-1}	0.002	0.100	−24.8	0.60
Trop. Rainforest (K34)/2000–2009				
NEE of CO_2 – µmol m^{-1} s^{-1}	0.004	−0.152	−15.7	0.27

* n indicate coefficients of the regression curve (Fig. 5).

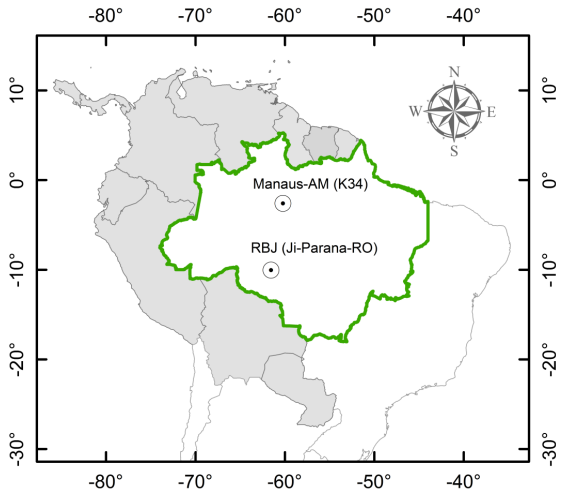

Fig. 1. Map of the study sites: Jaru Biological Reservation (RBJ), close to the city of Ji-Parana, Rondonia, Brazil and Cuieiras Biological Reservation (ZF-2, also called LBA tower K34), in Manaus, Amazonas, Brazil.

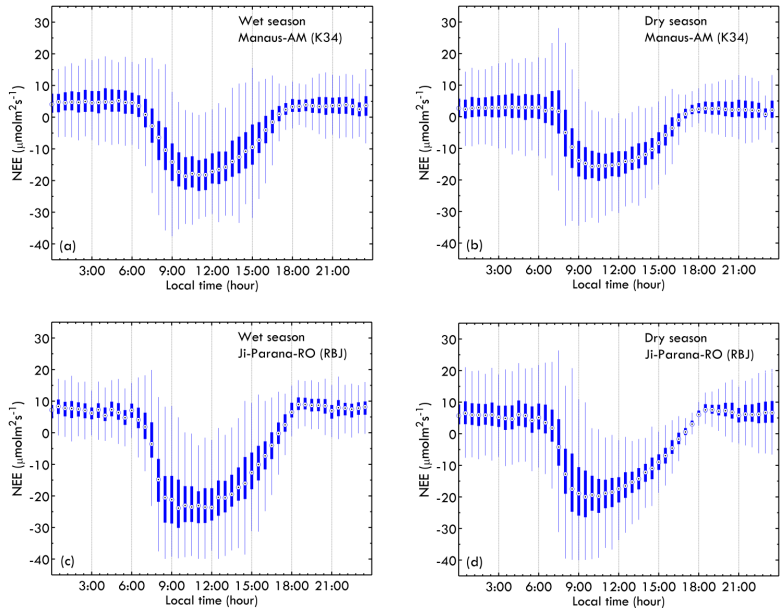

Fig. 2. Seasonally averaged diurnal cycles of NEE for the wet and dry seasons in the tropical rainforests in: **(a)** and **(b)** Manaus/K34 (1999–2009) and **(c)** and **(d)**: Ji-Parana/RBJ (1999–2002).

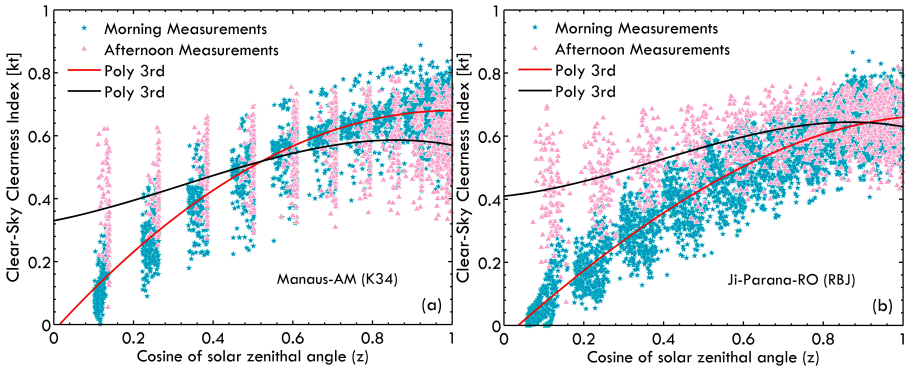

Fig. 3. Scatter plots and regressions between clear-sky clearness index and the cosine of solar zenithal angle for the K34 site near Manaus (2000–2009) **(a)** and for the RBJ site in Ji-Parana (2000–2002) **(b)**.

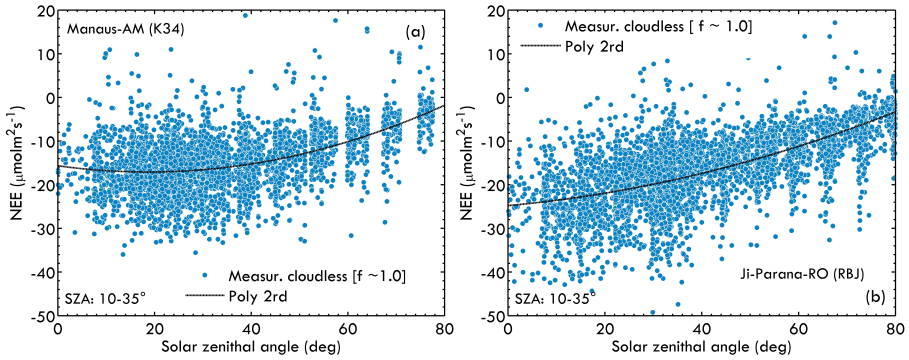

Fig. 4. Relationship between NEE and solar zenithal angle (SZA) for clear-sky conditions (f = 1.0) at the K34 **(a)**, for a poly 2rd fit with $R^2 = 0.27$ and $p < 0.01$, and at the RBJ **(b)**, for a poly 2rd fit with $R^2 = 0.60$ and $p < 0.001$.

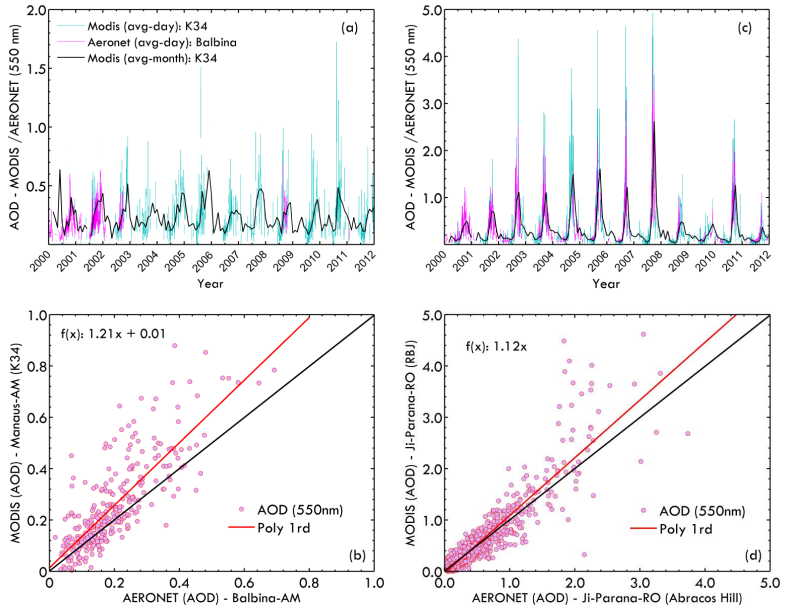

Fig. 5. Time series of AOD (at 550 nm) from 2000 to 2012 estimated by MODIS and measured by the AERONET sun photometer at 550 nm at the K34 site **(a)** and at the RBJ site **(c)**. **(b)** and **(d)** show regressions of the estimation of AOD by MODIS on the K34 sites **(b)** and at RBJ **(d)**. The red lines represent the linear fits at the both sites, with R^2 equal 0.64 (K34) and 0.84 (RBJ). The AOD values (AERONET) at 550 nm were calculated through Angström $\alpha \sim 1.01$ at the Balbina-AM **(b)** and $\alpha \sim 1.48$ at the Abracos Hill **(d)** sites. The differences between linear fit found between the estimates made by the MODIS (550 nm) and by sun photometer AERONET (500 nm) are less than ~ 5 % (not shown results).

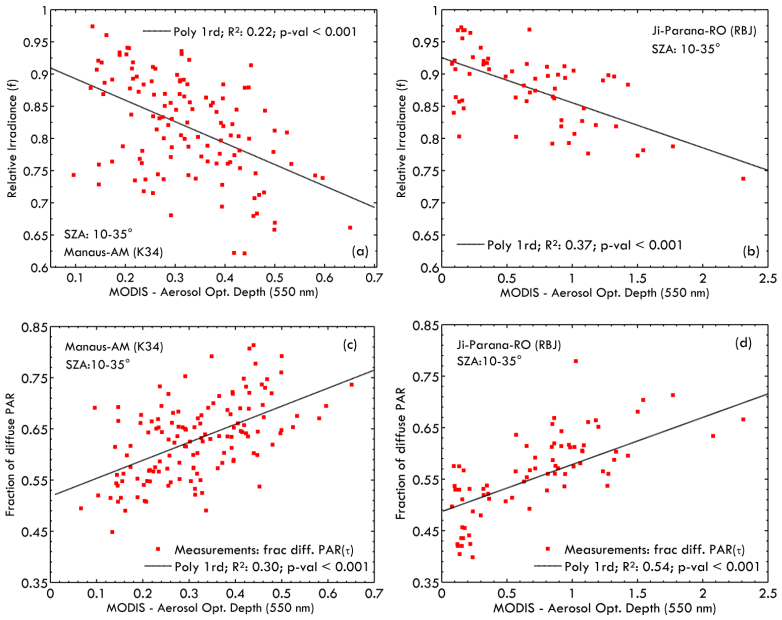

Fig. 6. Relationships between relative irradiance *f* and AOD (MODIS) for Manaus-K34 **(a)** and Ji-Parana (RBJ) **(b)**. The lower part shows the fraction of diffuse PAR for K34 **(c)** (2000–2009) and RBJ **(d)** (2000–2002).

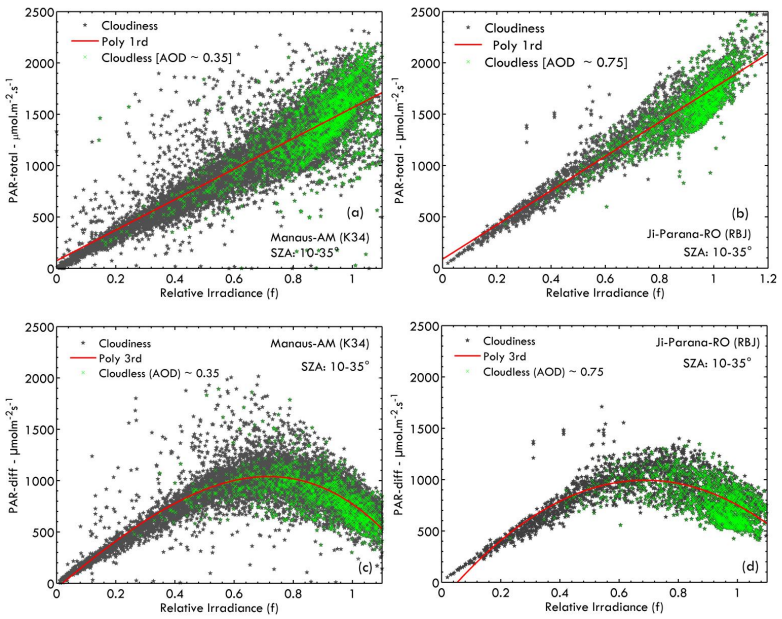

Fig. 7. Relationships between total PAR and relative irradiance *f* for the K34 site **(a)** and RBJ **(b)**. The lower part shows the diffuse PAR vs. relative irradiance *f* for K34 **(c)** and RBJ **(d)** sites. The period of the data used are: K34 site (2000–2009) and RBJ site (2000–2002).

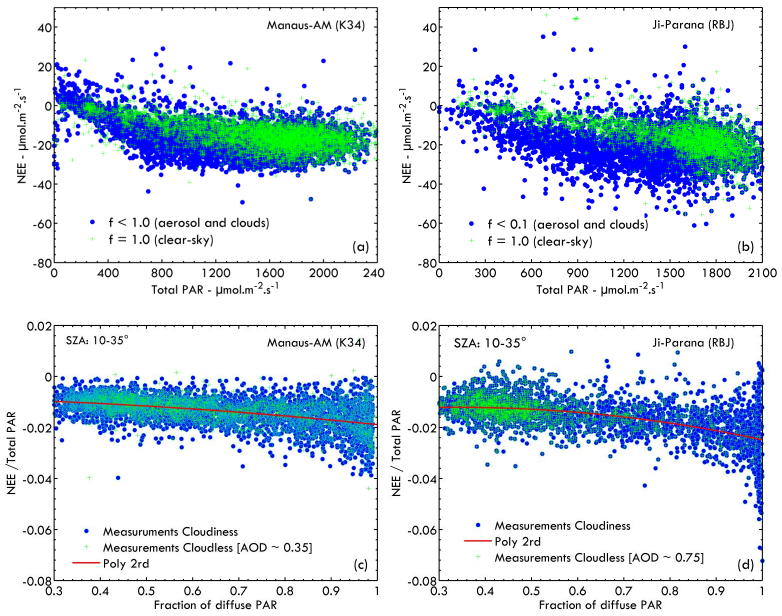

Fig. 8. NEE as a function of total downward PAR radiation for measurements between the 08:30 and 17:30 LT, for the K34 **(a)** and RBJ **(b)** sites. **(c)** and **(d)** shows the Light Use Efficiency (LUE) of vegetation as a function of the fraction of diffuse PAR at the K34 (R^2 = 0.21, p value < 0.001) in Manaus (2000–2009) **(c)** and RBJ (R^2 = 0.30, p value < 0.001) in Ji-Parana (2000–2002).

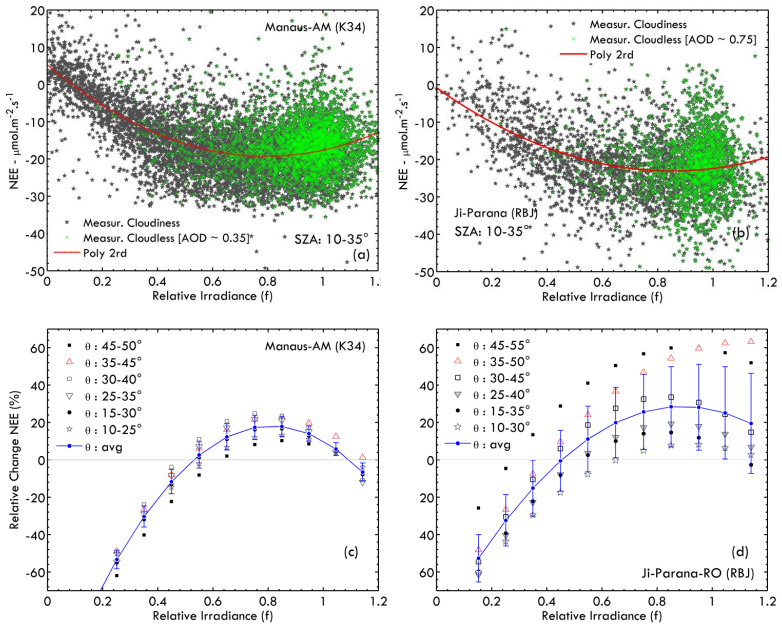

Fig. 9. Variability of NEE with the relative irradiance f for the K34/Manaus (R^2 = 0.32) and RBJ/Ji-Parana (R^2 = 0.12) sites for solar zenithal angle interval (z) between 10° and 35° **(a)** and **(b)**. Relative change of NEE (%NEE) as a function of the relative irradiance f, averaged for all solar zenithal angle intervals (z), from 10° to 55° **(c)** and **(d)**. Note that this plot includes clouds and aerosol effects.

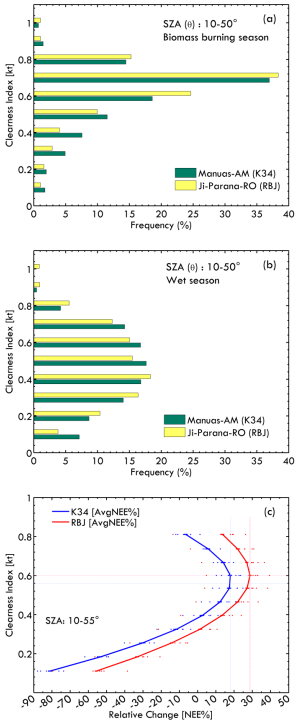

Fig. 10. Histograms of values of the clearness index for K34 and RBJ along the biomass burning season **(a)** and wet season **(b)**. The limit at which the cloudiness and/or aerosol load result in the maximum carbon uptake at RBJ and K34 are shown on the figure **(c)**. The relative change values (NEE%) were calculated for solar zenithal angles between 10° and 55°.

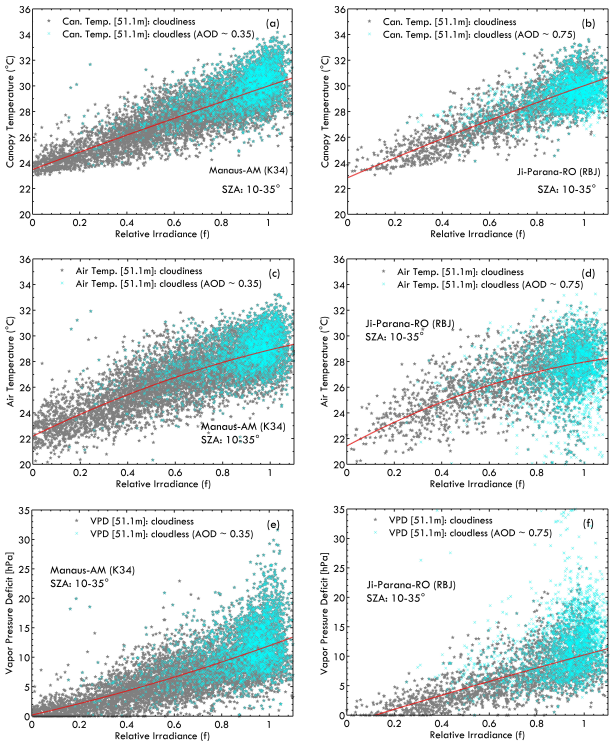

Fig. 11. Relationship between the relative irradiance parameter *f* with: **(a–b)** canopy temperature; **(c–d)** Air temperature and **(e–f)** Vapor Pressure Deficit. Values calculated for SZA between 10–35°. Air temperature was measured at 51.1 and 60.0 m over the ground in the K34 and RBJ, respectively.